Helicobacter pylori Vacuolating Toxin Forms Anion-Selective Channels in Planar Lipid Bilayers: Possible Implications for the Mechanism of Cellular Vacuolation

Francesco Tombola,* Cristina Carlesso,* Ildikò Szabò,* Marina de Bernard,* Jean Marc Reyrat,#
John L. Telford,# Rino Rappuoli,# Cesare Montecucco,* Emanuele Papini,* and Mario Zoratti*
*Centro CNR per lo Studio delle Biomembrane and Dipartimento di Scienze Biomediche, Università di Padova, Padova, Italy, and
#Centro di Ricerche I.R.I.S., CHIRON S.p.a., Siena, Italy

ABSTRACT The *Helicobacter pylori* VacA toxin plays a major role in the gastric pathologies associated with this bacterium. When added to cultured cells, VacA induces vacuolation, an effect potentiated by preexposure of the toxin to low pH. Its mechanism of action is unknown. We report here that VacA forms anion-selective, voltage-dependent pores in artificial membranes. Channel formation was greatly potentiated by acidic conditions or by pretreatment of VacA at low pH. No requirement for particular lipid(s) was identified. Selectivity studies showed that anion selectivity was maintained over the pH range 4.8–12, with the following permeability sequence: $Cl^- \approx HCO_3^- >$ pyruvate $>$ gluconate $> K^+ \approx Li^+ \approx Ba^{2+} > NH_4^+$. Membrane permeabilization was due to the incorporation of channels with a voltage-dependent conductance in the 10–30 pS range (2 M KCl), displaying a voltage-independent high open probability. Deletion of the NH_2 terminus domain (p37) or chemical modification of VacA by diethylpyrocarbonate inhibited both channel activity and vacuolation of HeLa cells without affecting toxin internalization by the cells. Collectively, these observations strongly suggest that VacA channel formation is needed to induce cellular vacuolation, possibly by inducing an osmotic imbalance of intracellular acidic compartments.

INTRODUCTION

The toxin VacA produced by pathogenic *Helicobacter pylori* strains is a major virulence factor in human gastroduodenal diseases (Warren and Marshall, 1983; Leunk et al., 1988; Cover and Blaser, 1992; Blaser, 1993; Eurogast Study Group, 1993; Parsonnet et al., 1994; Cover, 1997). The *vacA* gene, present in several homologous allelic forms in strains infecting different human populations (Cover, 1997), encodes for a 140-kDa precursor whose COOH terminal domain (40 kDa), necessary for extracellular secretion, is excised on the bacterial surface (Telford et al., 1994). The resulting mature 95-kDa toxin remains partly associated with the bacterial cell surface, but it is also released into the extracellular medium, as a low-activity complex formed by up to 12 subunits (Telford et al., 1994; Cover et al., 1997) Low-pH treatment strongly enhances the activity of VacA in model systems, presumably by causing oligomer disassembly (de Bernard et al., 1995; Cover et al., 1997; Reyrat et al., 1998).

Two different cellular effects mediated by VacA have been described so far: 1) alterations of the endocytic pathway (Papini et al., 1994; Molinari et al., 1997, 1998a; Satin et al., 1997) and 2) a size-selective increase of the permeability of polarized epithelial monolayers (Papini et al., 1998). In the first case, abnormally large V-ATPase-, rab7- and Igp-positive vacuoles develop in the cell cytoplasm from late endosomal and lysosomal compartments. Vacuolation is closely associated with pathogenicity, since VacA negative *H. pylori* strains are nonpathogenic.

Nothing is known about the molecular mechanism of VacA action. According to one hypothesis, VacA displays a catalytic activity in the cytosol, as A-B type toxins do (Menestrina et al., 1994). In these toxins the B domain/subunit is necessary for binding and for the translocation of the enzymatically active A portion. VacA is indeed formed by an N-terminal domain (p37) and a C-terminal domain (p58) linked by a protease-sensitive loop (Telford et al., 1994). The elimination of vacuolation by overexpression of dominant negative mutants of the small-GTP binding protein rab7 suggests that membrane traffic at the level of late endosomes is a necessary step in vacuole development (Papini et al., 1997). Vacuole induction by VacA expression in the cytosol of HeLa cells (de Bernard et al., 1997) is consistent with an enzymatic modification of a component regulating membrane traffic at the late stages of the endocytotic pathway.

However, other data suggest that VacA alters cellular ionic homeostasis in a still-unknown way. In fact, V-ATPase inhibitors prevent and revert the vacuolated phenotype, indicating that a pH gradient is necessary to form and maintain vacuolar vesicles (Papini et al., 1993), and the Na^+/K^+ ATPase inhibitor ouabain and permeable weak bases strongly enhance vacuole development (Cover and Blaser, 1992; Cover et al., 1993). These data suggest that changes in the cytosolic ion concentration and/or intraen-

Received for publication 21 September 1998 and in final form 7 December 1998.

Address reprint requests to Dr. Emanuele Papini, Dipartimento di Scienze Biomediche, Università di Padova, Viale G. Colombo n. 3, 35121 Padova, Italy, Tel.: +39 049 8276077; Fax: +39 049 8276049; E-mail: papinie@civ.bio.unipd.it.

Part of this work has already been presented as a meeting abstract [Tombola, F., C. Carlesso, E. Papini, C. Montecucco, and M. Zoratti. 1998. *Biophys. J.* 74:320a.

0006-3495/99/03/1401/09 $2.00

dosomal accumulation of osmotically active molecules play a crucial role in cell vacuolization by favoring water uptake and swelling of acidic compartments. One way in which VacA might induce osmotic unbalance is by forming channels in cell membranes. The connection between intracellular vacuolation and alterations of ion conductivity is not unprecedented, since monensin, a Na^+/H^+ ionophore, is known to induce Golgi swelling (Morre et al., 1988) and, more importantly, the bacterial protein toxin aerolysin, well-known to form oligomeric pores, causes ER vacuolation (Abrami et al., 1998). The hypothesis that VacA has a channel activity is supported by local homologies with ion pumps and transporters in the N-terminal region (Cover and Blaser, 1992), and by the report that the recombinant COOH terminal domain (p58) induced ion release from liposomes (Moll et al., 1995).

In the present work we report the characterization of voltage-dependent, anion-selective, low-conductance channels formed by native purified VacA in planar lipid membranes. Induction of channel activity is strongly enhanced by the exposure of VacA to low pH and correlates with the ability of VacA to induce intracellular vacuolation. Based on these data, it is proposed that an osmotic unbalance, induced by such channel activity, may contribute importantly to intracellular vacuolation. The possible role of the formation of anion-selective channels by VacA in *H. pylori* gastric infection is also discussed.

MATERIALS AND METHODS

Toxins and reagents

VacA was purified from *H. pylori* strain CCUG 17874, as described (Manetti et al., 1995), and stored at 0–4°C in phosphate-buffered saline (PBS) at the concentration of 0.1–0.2 mg/ml. The p58 VacA mutant construct results from an internal deletion within the p37 domain (amino acids 226–465) of the wild-type (wt) *vacA* gene of *H. pylori* strain 326 (Reyrat et al., in preparation). It was obtained using the counter selectable marker sacB (Copass et al., 1997). The resulting protein is secreted as a dimer isolated either through the standard procedure (Manetti et al., 1995) or by immunoaffinity isolation as described (Reyrat et al., 1998). N-terminal sequencing of the purified p58 showed that the remaining part of p37 was lost during isolation, most likely by protease cleavage, and that the actual NH_2 terminus started from the sequence GKGFN. Rabbit polyclonal antibody to native VacA was obtained as described (Manetti et al., 1995). Affinity purified Texas-red conjugated antibodies to rabbit IgG were from Jackson ImmunoResearch Laboratories, Inc. (West Grove, PA). Lipids: phosphatidyl-ethanolamine (PE) (from brain, purity >99%) and diphytanoyl-phosphatidylcholine (DPhPC) (synthetic, purity >99%) were purchased from Avanti Polar Lipids. Asolectin (Sigma type IIS or IVS, from soybean) was purified by acetone precipitation before use. Ganglioside GM1 was from Sigma. Diethylpyrocarbonate (DEPC; from Sigma) was handled as a solution in anhydrous ethanol. All other chemicals employed were of the highest purity available.

Planar lipid bilayer experiments

A home-made apparatus was used, following established techniques (Alvarez, 1986). The experiments were carried out basically as described (Szabò et al., 1998). Briefly, purified asolectin, DPhPC, or PE membranes with a capacity of ~300 pF were prepared by painting a decane or chloroform solution across a hole of ~300 μm diameter in a Teflon film separating two Teflon chambers (*cis* and *trans*). The content of the chambers could be stirred by magnetic bars. Connection to the electrodes was provided by agar bridges. Voltages of the *cis* side (side of toxin addition) are reported. Current (cations) flowing from the *cis* to the *trans* compartment are considered positive and plotted upward. The output of the amplifier was recorded on tape and analyzed off-line by using the pCLAMP 6.0 (Axon) program set. In most experiments (see Results for other protocols), VacA was pretreated by incubation in PBS/HCl, pH ≈ 2, 37°C, for 8–10 min immediately before use; 0.002–0.4 μg/ml toxin were used. The experimental medium was 100 or 500 mM KCl (or 2 M KCl for single channel recordings) plus 0.1 or 0.5 mM $CaCl_2$ and $MgCl_2$, 10 or 20 mM Hepes, pH 7.2, unless otherwise specified. For selectivity determinations either the composition of the medium in the *cis* chamber was changed after the appearance of VacA activity by substituting an aliquot with a more concentrated salt solution, or the toxin was added to the *cis* side directly under asymmetrical salt conditions. In experiments aimed at the construction of *I*/*V* curves for the determination of current reversal potentials (E_{rev}) (see Fig. 4) the raw current amplitude data were corrected for the continuing incorporation of channels during the experiment. We measured the current flowing at 0 mV at the beginning of each series of voltage pulses, and took this value as 100%. We then sequentially applied the desired voltages, with a short period at 0 mV separating periods at non-zero voltages. During this procedure VacA continued to incorporate, so that the current flowing at 0 mV increased in time. We measured this current immediately before the application of each pulse, and calculated the percent increase in the number of channels in the membrane from the ratio between this value and the initial one. We then decreased the measured value of the current conducted at the following non-zero potential by the same percentage. Depending on the experiment, the current increase over the whole sequence of pulses varied from zero to ~10%. In a few experiments we washed the *cis* chamber to eliminate the ongoing incorporation. The E_{rev} values from these experiments were the same within experimental error as those obtained by the procedure described. Polynomial interpolation of the experimental points was used to determine E_{rev}. Permeability coefficient ratios (Table 1) were calculated from E_{rev} values by applying the general current equation of the constant field theory (Hodgkin and Katz, 1949; Lewis, 1979), neglecting surface charge contributions. The latter were unimportant in our experiments since membranes made of neutral phospholipids (PE, DPhPC) were used in most such experiments, and essentially the same E_{rev} values were obtained when using asolectin instead. When constructing voltage-dependence plots, we measured the current conducted at a reference potential at the beginning and end of the voltage pulse series, and corrected the measured current amplitudes according to the difference between these values. We performed these determinations during the almost linear phase of current increase, or in the final plateau phase, and accordingly considered the increase to be proportional to the time-elapsed. Corrections were minor (0–5%).

DEPC modification

DEPC (5–400 μM final concentration) was added to a solution of nonactivated VacA (100 μg/ml in PBS, pH 7.4) or to a solution of VacA in PBS preactivated at pH 2.0 for 10 min and then neutralized. In this latter case acidification was achieved by adding 15 mM HCl, final concentration, to PBS and neutralization was obtained by adding 15 mM NaOH, final concentration. Reaction was blocked by 5 mM imidazole and VacA was diluted with Dulbecco's modified minimal essential medium (DMEM), supplemented with 10% fetal calf serum (FCS), and used to intoxicate cells. In the case of current measurements across planar lipid bilayers, VacA was preactivated and diluted in the *cis* chamber of the apparatus. After current development, DEPC was directly added to the chamber.

Cell culture and intoxication

HeLa cells were cultured on plastic flasks in complete DMEM supplemented with 10% FCS in a 5% (v/v) CO_2 atmosphere at 37°C. Before experiments, cells were suspended by trypsin-EDTA and seeded on 24-well standard titer plates or on glass coverslips at the density of 30,000/cm^2, cultured overnight, and treated for 3 h at 37°C with VacA (5–100 nM) diluted in DMEM medium, plus 2% FCS and 5 mM NH_4Cl. Vacuole formation was measured by the neutral red uptake assay (Cover and Blaser, 1992): cells were washed with PBS containing BSA 0.3% (w/v), and further incubated at room temperature with neutral red 8 mM in the same medium. After washing with PBS, neutral red was extracted with acidified 70% ethanol and quantified by measuring absorbance at 405 nm.

Indirect immunofluorescence microscopy

Cells on coverslips were washed with PBS, fixed with 3% paraformaldehyde in PBS for 20 min at room temperature, treated with 0.27% NH_4Cl, 0.38% glycine for 10 min, and permeabilized with 0.2% saponine, 0.5% BSA in PBS for 30 min. Primary antibodies to VacA were diluted in the permeabilization medium and applied to cells for 1 h. After several washes, Texas red-conjugated secondary antibodies were added, incubated for a further 30 min in the same medium, and then washed. Samples were mounted in 90% glycerol, 0.2% *N*-propylgallate in PBS, and microphotographed using a camera-equipped fluorescence microscope (Zeiss Axioplan).

RESULTS

pH-Dependent increase of bilayer conductance by VacA

The study of planar lipid bilayer permeabilization by toxins is a sensitive way to screen for and characterize their ion channel activity in vitro. Furthermore, several studies have shown that pore formation as revealed in model membranes is also displayed, with similar features, by toxins in the plasma membrane of living cells (Menestrina, 1991). The addition of purified, non-acid-activated VacA to the medium bathing a planar lipid bilayer resulted in only a slow increase of the membrane permeability to ions when the pH of the solution was close to neutrality. Shifting the medium pH to lower values in the VacA-containing (*cis*) compartment resulted in a marked current increase. The current versus time traces in Fig. 1, *A* and *B* illustrate this behavior, consistently observed in 13 experiments. Addition of non-acid-activated VacA to an acidic (pH 4.5–4.8) medium similarly resulted in a marked increase in the current conducted (not shown; $n = 7$). A strong bilayer conductance increase could be reproducibly obtained ($n > 180$) by incubating the VacA sample at low (2–4.5) pH for a few minutes before addition to the neutral medium (Fig. 1 *C*). This activation procedure was adopted in all other experiments. Toxin denatured by heating at 100°C was not active (not shown). In all cases, the current increase was preceded by a lag time of minutes, which varied considerably from experiment to experiment. As shown in Fig. 1, *A* and *C*, the current increased in sigmoidal fashion. The rate of current increase and the plateau level tendentially reached were roughly proportional to the amount of protein added (not shown), with some variability from experiment to experiment, which can be at least partially accounted for by differences in the area of the bilayer membrane. VacA-induced conductance increase with the characteristics exemplified in Fig. 1 was observed with membranes composed of asolectin, PE, and DPhPC, as well as with PE membranes containing up to 5% (w/w) ganglioside GM1 (with or without cholesterol) and with PE or asolectin membranes containing up to 3% cholesterol. The composition of the planar membrane had no identifiable influence on any of the characteristics of current development (not shown).

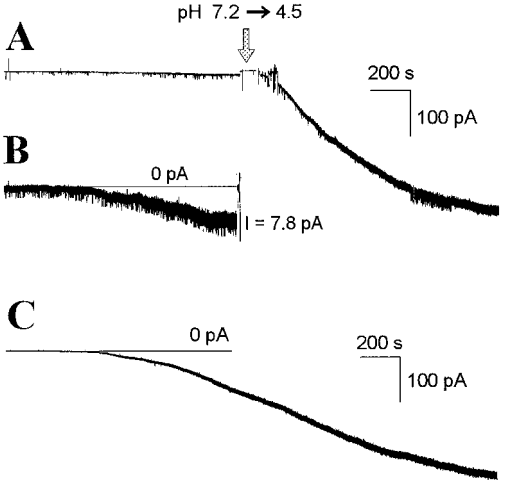

FIGURE 1 Current conduction by VacA. Activation by low pH. (*A*) Current conduction by a VacA-doped bilayer is strongly enhanced by acidification of the *cis* compartment. In the example shown, 200 ng/ml non-acid-activated VacA were added to the pH 7.2 medium, which was acidified after ~20 min by addition of HCl (*arrow*). Medium (*cis* and *trans* chambers): 500 mM KCl, 0.5 mM $CaCl_2$, 0.5 mM $MgCl_2$, 10 mM Hepes, 10 mM citrate/K, pH 7.2. Membrane: DPhPC. V(*cis*): −40 mV. Filter: 500 Hz. Digital sampling: 200 Hz. (*B*) The first part of the trace in (*A*) (before acidification), plotted with a 10-fold higher vertical (current) amplification. (*C*) A recording illustrating current conduction induced by VacA (27 ng/ml final concentration) preexposed to low pH. VacA was incubated for 8 min at 37°C in PBS/HCl, pH 1.9, before addition to the bilayer chamber. Medium: as in (*A*), minus citrate/K. Membrane: PE. V(*cis*): −40 mV. Filter: 500 Hz. Digital sampling: 200 Hz.

The current-voltage characteristic of VacA-doped membranes was non-Ohmic, as illustrated by the *I/V* curves in Fig. 2, *A* and *B*. A limited but clear rectification was observed, with less current flowing at positive (*cis*) potentials. This behavior can be more easily appreciated in the plots presented in Fig. 2 *C*, in which the ratio (I^+/I^-) of transbilayer current intensities at potentials of equal absolute value ($|V|$) but opposite sign is plotted versus $|V|$. The existence of a voltage dependence implies that the channels (see below) formed by VacA are intrinsically asymmetric and that they insert into the membrane with a preferred orientation. It is relevant that the form of the *I/V* relationship depended on the composition of the medium, with a more marked rectification in the pyruvate medium. This suggests that voltage variations affect the conductance of the pore, rather than its open probability (Eisenman and Horn, 1983), as confirmed by single-channel analysis (see below). Be-

sides influencing in this manner the conductance of the VacA-doped bilayer, the applied transmembrane voltage also affected the rate of current development, as shown in Fig. 2 *D*. This dependence was not just a reflection of the effect of voltage on the conductance of the channels (Fig. 2, *A–C*, Fig. 3 *G*), because it was considerably more pronounced than the latter (not shown). Rather, it represents largely a kinetic effect on the rate of channel incorporation into the planar membrane. This type of behavior can be understood if pore insertion implies the translocation across (part of) the transmembrane electrical field of a net negative charge.

VacA forms low-conductance voltage-dependent channels

The increase in bilayer conductance was due to the incorporation of bona fide low-conductance ion channels, whose gating could only be observed, with our setup, in the initial stages of the phenomenon (i.e., with only a few channels present) and in high-salt media. Fig. 3, *A–D* show representative single-channel traces indicating that these pores gate between open and closed state(s). The open probability of the channels was not influenced by the applied voltage within a given experiment, but varied between different experiments for unknown reasons. Both these aspects are illustrated in Fig. 3, *E* and *F*. These panels present current amplitude histograms from single-channel trace segments recorded in 2 M KCl at +40 and −40 mV. The histograms can be fitted as the sum of two Gaussian distributions. One, centered at 0 pA, originates from the baseline current (channel closed), while the other is due to the current flowing through the open channel. The areas under the two curves are therefore proportional to the time spent by the channel in the closed or open state(s), respectively. The relative size of the two components is not affected by the applied voltage (compare the histograms at +40 and −40 mV within a panel), but can differ in different experiments (compare panels *E* and *F*). These different gating behaviors can also be appreciated in the exemplificative current traces presented in panels *A–D*, which originate from four different experiments (compare traces *A* and *B* and traces *C* and *D*). While the applied voltage did not influence the open probability of the single channels, it did affect their mean conductance. This property is illustrated in Fig. 3 *G*, which plots the single-channel conductance (the current at the peak of the Gaussian fitted to the corresponding current amplitude histogram, divided by the applied voltage) versus voltage.

VacA pores are anion-selective

In experiments conducted under asymmetric ionic conditions (see Materials and Methods) we determined the relative permeabilities of VacA-doped membranes to a number of ionic species at 0 mV. Fig. 4 shows two representative

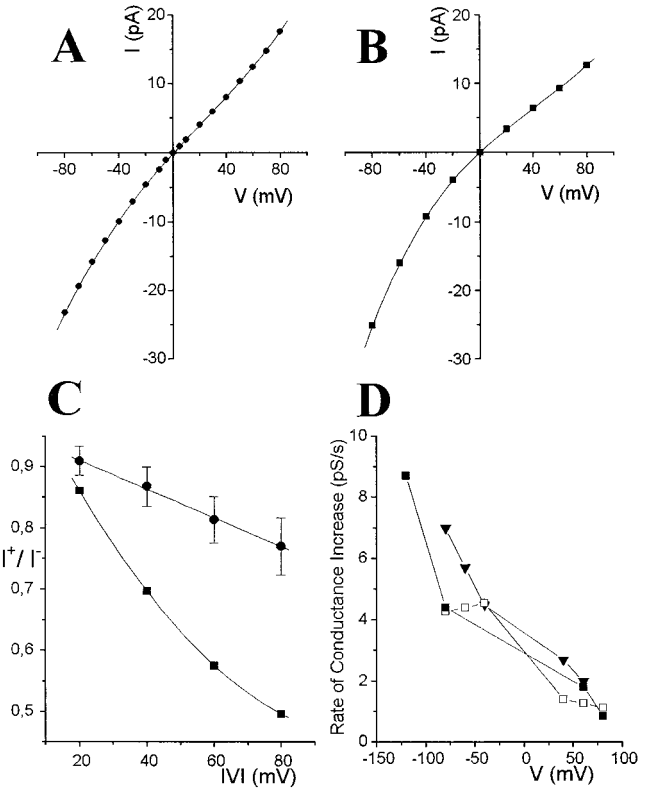

FIGURE 2 Voltage dependence of current conduction by VacA-doped bilayers. (*A* and *B*). Exemplificative *I/V* relationships. (*A*) Medium: 100 mM KCl, 0.5 mM $CaCl_2$, 0.5 mM $MgCl_2$, 10 mM Hepes, pH 7.2 (both chambers). Membrane: asolectin. (*B*) Medium: 100 mM K/pyruvate, 0.1 mM $CaCl_2$, 0.1 mM $MgCl_2$, 5 mM Hepes, pH 7.2 (both chambers). Membrane: PE. (*C*) The amplitude of the current flowing at applied positive (*cis*) potentials (I^+) was measured and divided by the amplitude conducted at the opposite (negative) potentials (I^-). Averages of these ratios are plotted versus the absolute value of the voltage ($|V|$). (●) KCl (100 or 500 mM) medium, $n = 11$. Error bars: standard deviations. (■) 100 mM K/pyruvate medium, $n = 2$. The average deviation was smaller than the size of the symbol used. (*D*) Effect of the applied voltage on the rate of bilayer conductance increase (channel incorporation). The approximate rate of conductance increase [$\Delta I/(V \times \Delta t)$] was measured at various applied voltages in the semilinear (central) part of the sigmoidal current versus time curve, and plotted versus voltage. Data from three separate experiments are shown. Membrane: asolectin. Medium as in (*A*).

I/V curves obtained with KCl and K-pyruvate media, while Table 1 summarizes the data collected. Permeation by anions is favored with respect to cations, even in the case of relatively bulky species such as pyruvate and gluconate. The permeability sequence deduced from these data is Cl^-, HCO_3^- > pyruvate > D-gluconate > K^+, Li^+, Ba^{2+} > NH_4^+. We furthermore determined that the P_{Cl}/P_K ratio is not appreciably affected by membrane composition (Asolectin, PE, DPhPC) and by pH in the range 4.8–12 (not shown). Of the 19 experiments aimed at the determination of the P_{Cl}/P_K ratio summarized in Table 1, three were conducted at pH 4.8, 7 at pH 7.2, 6 at pH 8.0, 2 at pH 10, and 1 at pH 12. This pH independence suggests that selectivity is determined by residues with $pK_a > 12$, presumably arginine.

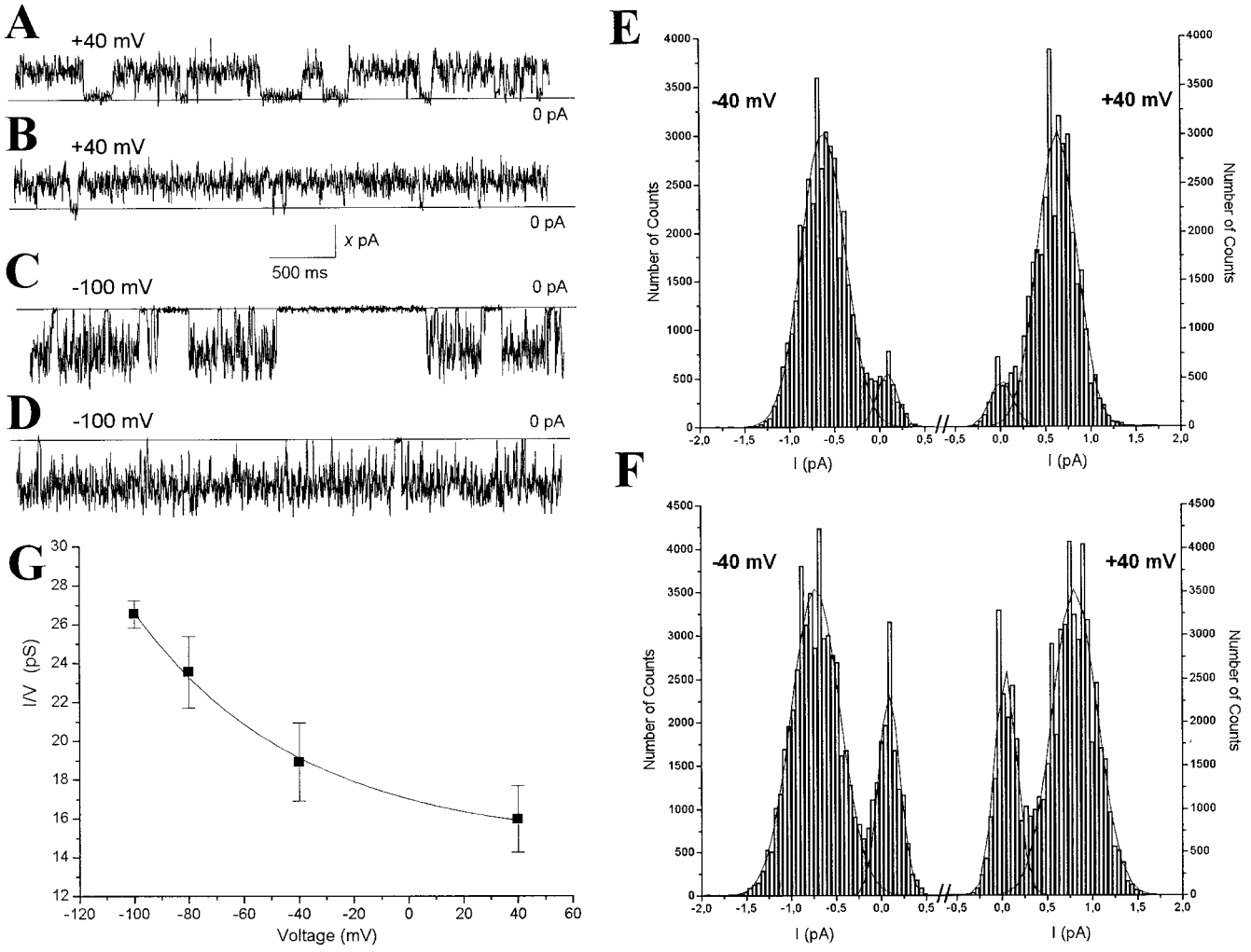

FIGURE 3 VacA pores. (*A–D*): Current traces illustrating single-channel behavior (see text). The vertical bar in the scaling inset corresponds to 1 pA for traces *A* and *B* and to 2 pA for traces *C* and *D*. Filter: 100 Hz. Sampling: 2 KHz. (*E* and *F*) Current amplitude histograms illustrating the variability of the single-channel kinetic behavior and the lack of voltage dependence of the open probability (see text). Open probabilities calculated from the histograms: (*E*) (−40 mV): 0.91; (+40 mV): 0.92; (*F*) (−40 mV): 0.78; (+40 mV): 0.73. (*G*) The averages of five to seven determinations of single channel conductance at various voltages, based on current amplitude histogram fits (peak values), are plotted versus *V*. Error bars: standard deviations. All panels: membrane: DPhPC; medium: 2 M KCl, 0.5 mM $CaCl_2$, 0.5 mM $MgCl_2$, 10 mM Hepes, pH 7.2.

VacA p58 shows no channel-forming activity

Based on the possibility that VacA might be an A-B-type toxin (see Introduction) we tested the ability of the mutated construct VacA p58 (corresponding to the C-terminal, possibly equivalent to a "B" toxin domain; see Materials and Methods) to induce an increase of planar bilayer permeability. p58 was purified by two different procedures (see Materials and Methods). All attempts to detect a channel-forming activity by this construct failed (Fig. 5; $n = 10$, employing various membrane and medium compositions and low-pH activation protocols). Wild-type VacA, purified according to the same protocols used for the p58 mutant, exhibited the usual behavior when added after p58 (Fig. 5) as well as in separate experiments (not shown). The same construct, when added to HeLa cells, bound to the cellular membrane but failed to induce vacuolization (J. M. Reyrat et al., manuscript in preparation).

Chemical modification of VacA with DEPC decreases both cell vacuolation and the conductance of toxin-doped bilayers

To collect further information on the functional role of VacA channels in vacuolation we used the histidine-modifying reagent diethylpyrocarbonate (DEPC). Preincubation of VacA with DEPC severely inhibited its ability to induce intracellular vacuoles in HeLa cells (Figs. 6, *A* and *C* and 7 *B*). Immunofluorescence analysis with specific antibodies to VacA showed that cell internalization into typical intracellular endocytic vesicles, and by inference also the interaction of VacA with the cell surface, were not affected by

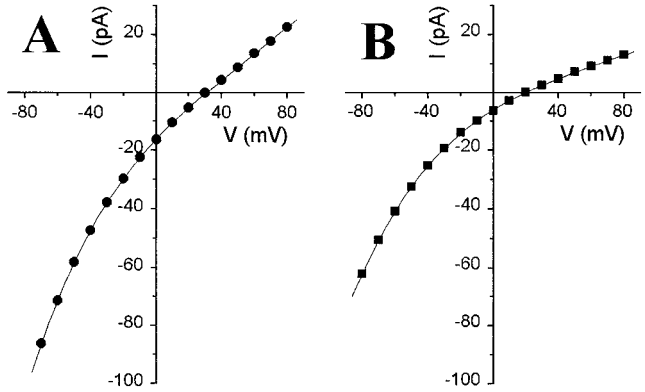

FIGURE 4 Reversal potential determinations. Representative *I/V* plots from two experiments aimed at the determination of E_{rev} with 390:100 (*cis:trans*) mM KCl (*A*) and K/pyruvate (*B*) (pH 7.2). The membrane was made of PE in both cases.

TABLE 1 Selectivity of VacA channels

Anion*	$[Salt]^{\S}_{cis}$ (mM)	E_{rev} (mV)	P_{anion}/P_{K^+} Ave ± SD	*n*
Cl^-	390	29–33	24 ± 10	19
HCO_3^-	461	32–35	21 ± 7	6
Pyruvate$^-$	390	19–20	5.8 ± 1.6	9
D-Gluconate$^-$	290	6.6–7.6	1.7 ± 0.1	4
Cation#			P_{Cl^-}/P_{cation}	
Li^+	390	29–31	17 ± 2	6
Ba^{2+}	542	20–21	17 ± 2	5
NH_4^+	390	33–34	67 ± 15	3

Current reversal potentials determined from plots like those presented in Fig. 4 were used to calculate permeability ratios at 0 mV. The range of E_{rev} is reported. The permeability ratios given are the averages of the values calculated from each experimentally determined E_{rev} ± SD.
*Cation was K^+.
#Anion was Cl^-.
§*trans* concentration was 100 mM.

DEPC treatment (Fig. 6, *B* and *D*). In planar bilayer experiments ($n = 11$), addition of DEPC (200–666 μM) to the medium bathing VacA-doped membranes reduced current conduction by as much as 75% (Fig. 7).

DISCUSSION

The characterization of membrane interactions is a central topic in the study of both plasma membrane- and cytosol-acting toxins. In the first case, toxicity is caused by alterations of the lipid bilayer permeability, while in the second, the translocation of a catalytic subunit into the cell cytosol is often accompanied by the formation of ion channels with no toxic action by themselves (Montecucco et al., 1992; Menestrina et al., 1994).

In the present paper we have shown for the first time that native VacA can form low-conductance, voltage-dependent, anion-selective channels in planar lipid bilayers. A linkage between pore formation and the ability of VacA to induce intracellular vacuolation is suggested by the following observations: channel activity is strongly enhanced by incubation or pretreatment at low pH, conditions which also boost cell vacuolation (de Bernard et al., 1995). No alteration of membrane permeability was detected using a vacuolation-inactive construct lacking the p37 domain. Chemical modification by DEPC strongly inhibits VacA-induced current conduction and parallely inhibits cellular vacuolation, without affecting cell binding and endocytosis.

Low pH induction of VacA channels can be explained by recent data: acidic pH induces the dissociation of vacuolation-inactive VacA oligomers into monomers (Cover et al., 1997) that expose hydrophobic surfaces allowing the interaction of both the aminoterminal (p37) and the carboxyterminal (p58) domains with the hydrophobic core of artificial lipid bilayers (Molinari et al., 1998b). Hence, it can be proposed that the formation of VacA channels requires the dissociation of the oligomer and the insertion of the released monomers into the membrane. The lag time characterizing current development in our experiments indicates that other events besides insertion are required. These might consist in the reassociation of monomers to form a current-conducting oligomeric structure either before membrane insertion or after insertion. In either case, the re-formed oligomer may be different from the original one, as previously suggested (de Bernard et al., 1995; Cover et al., 1997). The inability of VacA p58 to form channels in our system is unexpected if one assumes that VacA has an A-B type organization, with the N-terminal domain, p37, constituting the catalytic part, and the C-terminal domain, p58, representing the binding, channel-forming domain (Moll et al., 1995). This inability might depend on an altered conformation and/or oligomerization of this mutant or it might mean that regions of both p58 and p37 are required for proper channel assembly. This latter possibility is in agreement with hydrophobic photolabeling experiments showing the insertion in the lipid bilayer of both domains (Molinari et al., 1998b) and with the presence of a fairly hydrophobic aminoterminal segment in the VacA sequence (Cover and Blaser, 1992). Whatever

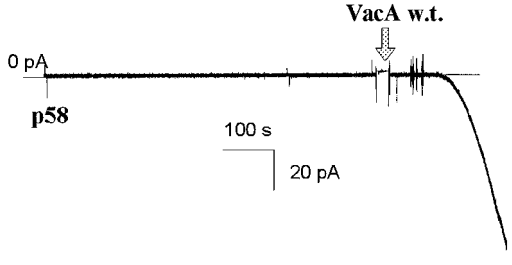

FIGURE 5 VacA p58 does not form pores. A representative experiment is shown. VacA p58 (300 ng/ml), pretreated at pH 2 for 8 min at 37°C, was added to the bilayer chamber 16 min before the beginning of the trace segment shown. After ~26 min from the start of the experiment, 333 ng/ml of wt/VacA, purified and activated in the same manner as VacA p58, were added (*arrow*). Membrane: asolectin. Medium as in Fig. 1 *C*. *V*: −40 mV; filter: 500 Hz. dig. sampling frequency: 100 Hz.

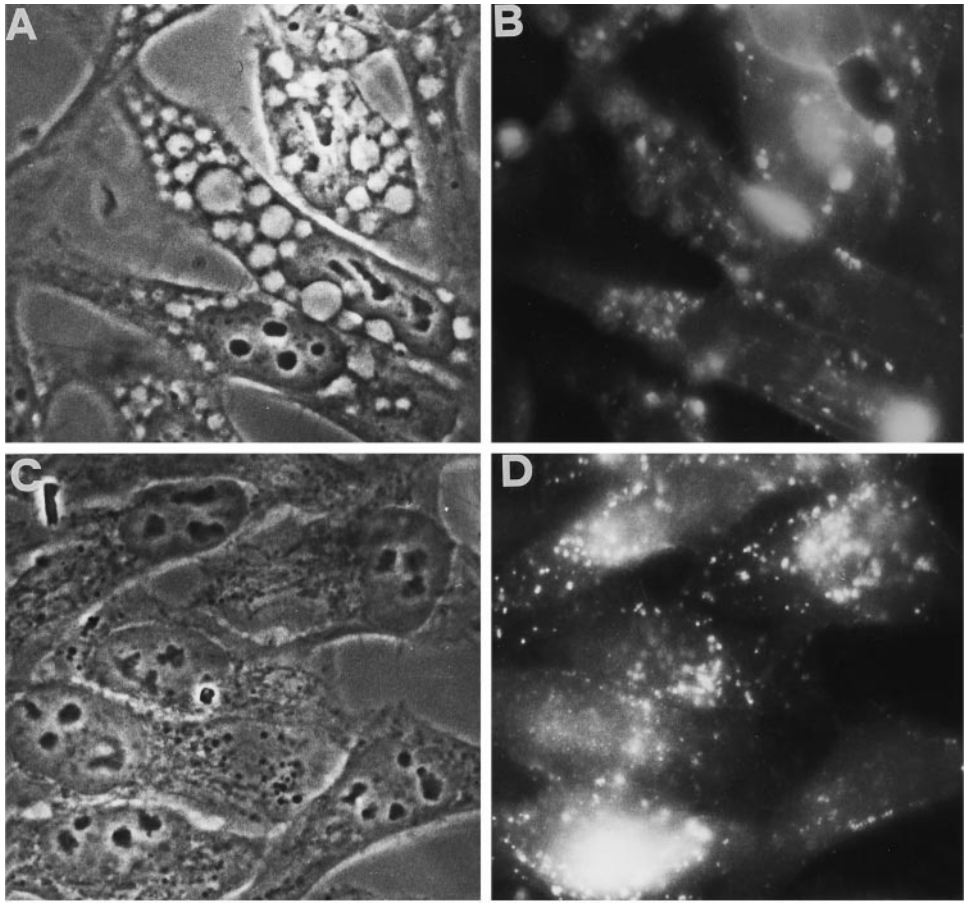

FIGURE 6 DEPC inhibits vacuolation by VacA, but not toxin internalization. HeLa cells were incubated at 37°C with VacA (10 μg/ml in DMEM, 10% FCS), pretreated (*C* and *D*) or not (*A* and *B*) with DEPC (100 μg/ml VacA in PBS, 400 μM DEPC, 25°C for 60 min) and then activated at pH 2.0 (see Methods). After 3 h, cells were fixed and processed for indirect immunofluorescence with antibodies to VacA and Texas-red-conjugated secondary antibodies. Microphotographs were obtained using an Axioplan fluorescence microscope (Zeiss). Magnification 350×. (*A* and *C*) Exemplificative phase-contrast images of fields of cells exposed to VacA (*A*) or to DEPC-treated VacA (*C*). (*B* and *D*): Immunofluorescence images of the same fields as in (*A*) and (*C*), respectively.

the explanation, the results suggest that a loss of the ability of inducing channels is associated with impairment of vacuolation.

How might pore formation be related to VacA cytotoxicity? As mentioned, it might just be a consequence of the engagement of the membrane core necessary for the translocation of the putative active domain into the cytosol. Indeed, the fluctuations displayed by VacA channels (Fig. 3) resemble those of pores formed by A-B-type toxins. However, this similarity does not necessarily imply analogies in the mechanism of toxin action. The data collected in this work are also consistent with the alternative possibility that the cytotoxic action of VacA is caused or is at least strongly enhanced by the channel activity itself. VacA may form anion-selective channels, after endocytosis, in the membrane of endocytic compartments where it might well be activated by the acidic conditions. In fact, VacA is endocytosed (Garner and Cover, 1996) and found to be localized in V-ATPase-positive vesicles (our unpublished results) and vacuoles (Papini et al., 1996; Ricci et al., 1997). The expected increase in ion conductivity of the endosomal membrane is predicted to enhance the turnover of the electrogenic V-ATPase (Galloway et al., 1983; Van Dyke, 1986; Nelson, 1992), leading to a higher influx of H^+ and Cl^- from the cytosol into the endosomal lumen. As a result, membrane-permeant amines, known to accelerate VacA-induced vacuolation (Cover and Blaser, 1992; Papini et al., 1996) would accumulate in the lumen because of the pH gradient and because VacA channels are poorly permeable to the corresponding protonated species (see Table 1 for NH_4^+). This would be expected to lead to secondary water influx and swelling (Fig. 8). This model is in agreement with the essential role of the V-ATPase, whose inhibition leads to impairment and reversal of vacuolation (Cover et al., 1993; Papini et al., 1993). In the absence of permeant amines, the effects of VacA channels on osmotic balance are less easy to predict, because the pores have a finite, although low, permeability also to physiological cations such as Na^+ and K^+. However, some osmotic swelling of VacA-containing endosomes is likely to take place even under these conditions, as suggested by electron microscopy (Ricci et al., 1997). Despite the presence of abundant membrane invaginations in late endosomes (Griffiths, 1996), osmotic swelling by itself can hardly account for the formation of vacuolar structures of up to 5 μm in diameter. Indeed, the supply of membrane from early endosomes and endosomal homotypic fusion are necessary for the formation of large vacuoles (Papini et al., 1997).

To explain the observation that expression of VacA in the cell cytosol leads to vacuolation, the mechanistic model of Fig. 8 must postulate that the cytosolic toxin retains the ability to form anion-selective channels in the membranes

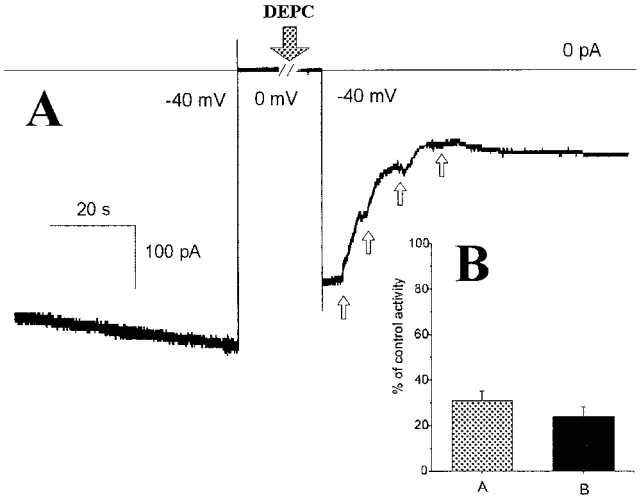

FIGURE 7 DEPC inhibits current conduction by VacA-doped bilayers. (*A*) The trace from an experiment in which 400 μM DEPC was added to the *cis* chamber (*downward arrow*) in the course of a standard experiment with preactivated VacA is shown as an example. Upward arrows denote stirring of the chamber contents, progressively leading to homogenization of reactant concentration. The break in the trace, lasting 28 s, corresponds to DEPC addition. Medium as in Fig. 1 *C*. Membrane: asolectin; filter: 500 Hz; dig. sampling: 200 Hz. (*B*) Column A (*gray*): the percentage ± SD current remaining after the addition of 400 μM DEPC in experiments as exemplified in (*A*) ($n = 6$). Column B (*black*): the percent inhibition of vacuolation induced by treatment of VacA with 200 μM DEPC, in experiments as exemplified in Fig. 6 ($n = 3$). Vacuolation was quantified by neutral red uptake (see Methods).

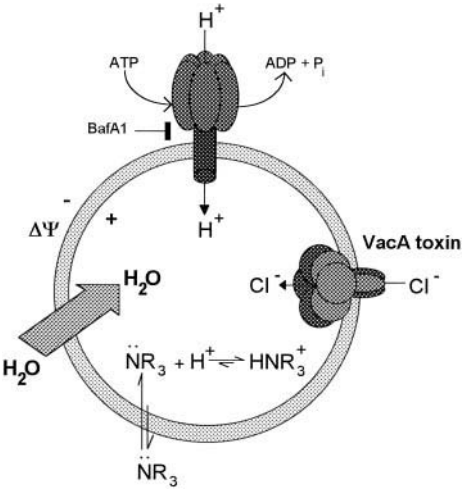

FIGURE 8 The possible effect of VacA on ion homeostasis of acidic compartments. The model envisages the possible consequences of the formation of anion-selective channels in the membrane of endosomes of intoxicated cells. Endocytosed VacA channels would stimulate the H^+ pumping activity of the V-ATPase by increasing the permeability of the endosomal membrane to anions. Following weak base ($R\text{-}NH_2$) permeation, osmotically active species accumulate in the endosomal lumen, leading to water influx from the cytosol.

of acidic compartments. This hypothesis is consistent with the observation that VacA immunoreactivity in transfected cells associates with V-ATPase-containing compartments undergoing vacuolation (de Bernard et al., 1997).

The hypothesis of a VacA-dependent osmotic unbalance as a major factor in cellular vacuolation raises the question of the biological meaning of the presently described channel activity and of its role in the pathogenesis of gastritis and ulcers. The selectivity determinations performed in this work show that anions such as Cl^-, HCO_3^-, and small organic molecules (e.g., pyruvate) are conducted by VacA channels. Based on these data, we propose that VacA might be part of an *H. pylori* strategy to survive on the surface of the gastric epithelium by extracting nutrients from the host cells. Bound *H. pylori* cells might use VacA to locally permeabilize the apical membrane of gastric epithelial cells and generate an efflux of HCO_3^- and other readily usable substrates (Mendz et al., 1994). In this respect it is worth noticing that the concentration of CO_2 is critical for *H. pylori* growth (Burns et al., 1995). The VacA-induced increase of epithelial permeability to small organic molecules and to ions (Papini et al., 1998) might serve the same purpose, i.e., nutrient supply. Vacuolation might be the late consequence of this increase in anion permeation. In fact, vacuolation requires a long time to develop in the absence of permeable weak bases, while other functional effects such as inhibition of endosomal functions, lysosomal markers redistribution, and change in epithelial permeability appear before or in the absence of vacuoles.

To conclude: we described and characterized a new property of VacA, the ability to form anion-selective channels in lipid bilayers, which leads to a model of intracellular vacuole formation consistent with available observations. This hypothesis postulates an increased delivery of osmotically active ions to the lumen of late endosomes, supported by V-ATPase activity. We propose that the actual aim of such activity is not cellular vacuolation but, rather, the induction of an increased efflux of HCO_3^- and anionic metabolites from the stomach mucosa (Blaser, 1993; Papini et al., 1998).

We thank Dr. G. Bàthori for performing the initial experiments, Dr. B. Satin for help with toxin purification, and Drs. Sandra Brutsche and Vladimir Pelicic for helpful criticisms.

This work was supported by EC Grants (TMR FMRX CT96 0004 and Biomed BMH4 CT97 2410), by Murst ex60% and, ex40%, by a research grant from the Giovanni Armenise-Harvard Foundation for Advanced Science, by the CNR Target project on Biotechnology 97.01168 PF 49, and it has been carried out in part under a research contract with Consorzio Autoimmunità Tardiva C.A.U.T., Pomezia, Italy, within the "Programma Nazionale Farmaci-seconda fase" of the Italian Ministry of the University and Scientific and Technological Research. We are also particularly grateful to Telethon-Italy for financial support (grants A.44 and A.59 to M.Z.). I.S. held a postdoctoral fellowship from the University of Padova.

This work is in partial fulfillment of the Doctorate degree in Cellular and Molecular Biology and Pathology of the University of Padova by Francesco Tombola.

REFERENCES

Abrami, L., M. Fivaz, P. E. Glauser, R. G. Parton, and F. G. van der Goot. 1998. A pore-forming toxin interacts with a GPI-anchored protein and

causes vacuolation of the endoplasmic reticulum. *J. Cell Biol.* 140: 525–540.

Alvarez, O. 1986. How to set up a bilayer system. *In* Ion Channel Reconstitution, C. Miller, editor. Plenum Press, New York and London. 115–130.

Blaser, M. J. 1993. *Helicobacter pylori:* microbiology of a "slow" bacterial infection. *Trends Microbiol.* 1:255–259.

Burns, B. P., S. L. Hazell, and G. L. Mendz. 1995. Acetyl-CoA carboxylase activity in *Helicobacter pylori* and the requirement of increased CO_2 for growth. *Microbiology.* 141:3113–3118.

Copass, M., G. Grandi, and R. Rappuoli. 1997. Introduction of unmarked mutations in the *Helicobacter pylori* vacA gene with a sucrose sensitivity marker. *Infect. Immun.* 65:1949–1952.

Cover, T. L. 1997.The vacuolating cytotoxin of *Helicobacter pylori. Mol. Microbiol.* 20:241–246.

Cover, T. L., and M. J. Blaser. 1992. Purification and characterization of the vacuolating toxin from *Helicobacter pylori. J. Biol. Chem.* 267: 10570–10575.

Cover, T. L., P. I. Hanson, and J. E. Heuser, 1997. Acid-induced dissociation of VacA, the *Helicobacter pylori* vacuolating toxin, reveals its pattern of assembly. *J. Cell Biol.* 138:759–769.

Cover, T. L., L. Y. Reddy, and M. J. Blaser. 1993. Effects of ATPase inhibitors on the response of HeLa cells to *Helicobacter pylori* vacuolating toxin. *Infect. Immun.* 61:1427–1431.

de Bernard, M., B. Arico', E. Papini, R. Rizzuto, G. Grandi, R. Rappuoli, and C. Montecucco. 1997. *Helicobacter pylori* toxin VacA induces vacuole formation by acting in the cell cytosol. *Mol. Microbiol.* 26: 665–674.

de Bernard, M., E. Papini, V. de Filippis, E. Gottardi, J. L. Telford, R. Manetti, A. Fontana, R. Rappuoli, and C. Montecucco. 1995. Low pH activates the vacuolating toxin of *Helicobacter pylori*, which becomes acid and pepsin resistant. *J. Biol. Chem.* 270:23937–23940.

Eisenman, G., and R. Horn. 1983. Ionic selectivity revisited: the role of kinetic and equilibrium processes in ion permeation through channels. *J. Membr. Biol.* 76:197–225.

Eurogast Study Group. 1993. An international association between *Helicobacter pylori* infection and gastric cancer. *Lancet.* 341:1359–1362.

Galloway, C. J., G. E. Dean, M. Marsh, G. Rudnick, and I. Mellman. 1983. Acidification of macrophage and fibroblast endocytic vesicles in vitro. *Proc. Natl. Acad. Sci. USA.* 80:3334–3338.

Garner, J. A., and T. L. Cover. 1996. Binding and internalization of the *Helicobacter pylori* vacuolating cytotoxin by epithelial cells. *Infect. Immun.* 46:4197–4203.

Griffiths, G. 1996. On vesicles and membrane compartments. *Protoplasma.* 195:37–58.

Hodgkin, A., and B. Katz. 1949. The effect of sodium ions on the electrical activity of the giant axon of the squid. *J. Physiol.* 108:37–77.

Leunk, R. D., P. T. Johnson, B. C. David, W. G. Kraft, and D. R. Morgan. 1988. Cytotoxin activity in broth-culture filtrates of *Campylobacter pylori. J. Med. Microbiol.* 26:93–99.

Lewis, C. A. 1979. Ion-concentration dependence of the reversal potential and the single channel conductance of ion channels at the frog neuromuscular junction. *J. Physiol.* 286:417–445.

Manetti, R., P. Massari, D. Burroni, M. de Bernard, A. Marchini, R. Olivieri, E. Papini, C. Montecucco, R. Rappuoli, and J. L. Telford. 1995. *Helicobacter pylori* cytotoxin: importance of native conformation for induction of neutralizing antibodies. *Infect. Immun.* 63:4476–4480.

Mendz, G. L., S. L. Hazell, and L. van Gorkom. 1994. Pyruvate metabolism in *Helicobacter pylori. Arch. Microbiol.* 162:187–192.

Menestrina, G. 1991. Electrophysiological methods for the study of toxin-membrane interaction. *In* Sourcebook of Bacterial Protein Toxins. J. E. Alouf and J. H. Freer, editors. Academic Press, London. 45–56.

Menestrina, G., G. Schiavo, and C. Montecucco. 1994. Molecular mechanisms of action of bacterial protein toxins. *Molec. Aspects Med.* 15: 79–193.

Molinari, M., C. Galli, N. Norais, J. L. Telford, R. Rappuoli, J. P. Luzio, and C. Montecucco. 1997. Vacuoles induced by *Helicobacter pylori* toxin contain both late endosomal and lysosomal markers. *J. Biol. Chem.* 272:25339–25344.

Molinari, M., C. Galli, M. de Bernard, N. Norais, J. M. Ruysschaert, R. Rappuoli, and C. Montecucco. 1998b. The acid activation of *Helicobacter pylori* toxin VacA: structural and membrane binding studies. *Biochem. Biophys. Res. Commun.* 248:334–340.

Molinari, M., M. Salio, C. Galli, N. Norais, R. Rappuoli, A. Lanzavecchia, and C. Montecucco. 1998a. Selective inhibition of Li-dependent antigen presentation by *Helicobacter pylori* toxin VacA. *J. Exp. Med.* 187: 135–140.

Moll, G., E. Papini, R. Colonna, D. Burroni, J. L. Telford, R. Rappuoli, and C. Montecucco. 1995. Lipid interaction of the 37-kDa and 58-kDa fragments of the *Helicobacter pylori* cytotoxin. *Eur. J. Biochem.* 234: 947–952.

Montecucco, C., E. Papini, G. Schiavo, E. Padovan, and O. Rossetto. 1992. Ion channel and membrane translocation of diphtheria toxin. *FEMS Microbiol. Immun.* 105:101–112.

Morre, D. J., N. Minnifield, and H. H. Mollenhauer. 1988. Kinetics of monensin-induced swelling of Golgi apparatus cisternae of H-2 hepatoma cells. *Eur. J. Cell Biol.* 37:107–110.

Nelson, N. 1992. Organellar proton-ATPases. *Curr. Opin. Cell. Biol.* 4:654–660.

Papini, E., M. Bugnoli, M. de Bernard, N. Figura, R. Rappuoli, and C. Montecucco. 1993. Bafilomycin A1 inhibits *Helicobacter pylori*-induced vacuolization of HeLa cells. *Mol. Microbiol.* 7:323–327.

Papini, E., M. de Bernard, E. Milia, M. Bugnoli, M. Zerial, R. Rappuoli, and C. Montecucco. 1994. Cellular vacuoles induced by *Helicobacter pylori* originate from late endosomal compartments. *Proc. Natl. Acad. Sci. USA.* 91:9720–9724.

Papini, E., E. Gottardi, B. Satin, M. de Bernard, J. Telford, P. Massari, R. Rappuoli, S. B. Sato, and C. Montecucco, 1996. The vacuolar ATPase proton pump is present on intracellular vacuoles induced by *Helicobacter pylori. J. Med. Microbiol.* 44:1–6.

Papini, E., B. Satin, C. Bucci, M. de Bernard, J. L. Telford, R. Manetti, R. Rappuoli, M. Zerial, and C. Montecucco. 1997. The small GTP binding protein rab7 is essential for cellular vacuolation induced by *Helicobacter pylori* cytotoxin. *EMBO J.* 16:15–24.

Papini, E., B. Satin, N. Norais, M. de Bernard, J. L. Telford, R. Rappuoli, and C. Montecucco, C. 1998. Selective increase of the permeability of polarized epithelial cell monolayers by *Helicobacter pylori* vacuolating toxin. *J. Clin. Invest.* 102:813–820.

Parsonnet, J., S. Hansen, L. Rodriguez, A. Gelb, A. Warnke, E. Jellum, N. Orentreich, J. Vogelman, and G. Friedman. 1994. *Helicobacter pylori* infection and gastric lymphoma. *N. Engl. J. Med.* 330:1267–1271.

Reyrat, J. M., M. Charrel, C. Pagliaccia, D. Burroni, P. Lupetti, M. de Bernard, J. Xuhai, N. Norais, E. Papini, R. Dallai, R. Rappuoli, and J. L. Telford. 1998. Characterization of a monoclonal antibody and its use to purify the cytotoxin of *Helicobacter pylori. FEMS. Microbiol. Lett.* 165:79–84.

Ricci, V., P. Sommi, R. Fiocca, M. Romano, E. Solcia, and U. Ventura. 1997. *Helicobacter pylori* vacuolating toxin accumulates within the endosomal-vacuolar compartment of cultured gastric cells and potentiates the vacuolating activity of ammonia. *J. Pathol.* 183:453–459.

Satin, B., N. Norais, J. L. Telford, R. Rappuoli, M. Murgia, C. Montecucco, and E. Papini. 1997. Effect of *Helicobacter pylori* vacuolating toxin on maturation and extracellular release of procathepsin D and on epidermal growth factor degradation. *J. Biol. Chem.* 272:25022–25028.

Szabò, I., G. Bàthori, F. Tombola, A. Coppola, I. Schmehl, M. Brini, A. Ghazi, V. De Pinto, and M. Zoratti. 1998. Double-stranded DNA can be translocated across a planar membrane containing purified mitochondrial porin. *FASEB J.* 12:495–502.

Telford, J. L., P. Ghiara, M. Dell'Orco, M. Comanducci, D. Burroni, M. Bugnoli, M. F. Tecce, S. Censini, A. Covacci, Z. Xiang, E. Papini, C. Montecucco, L. Parente, and R. Rappuoli. 1994. Purification and characterization of the vacuolating toxin from *Helicobacter pylori. J. Exp. Med.* 179:1653–1658.

Tombola, F., C. Carlesso, I. Szabò, E. Papini, C. Montecucco, and M. Zoratti. 1998. Electrophysiological properties of the *Helicobacter pylori* vacuolating toxin, VacA. *Biophys. J.* 74:320a.

Van Dyke, R. W. 1986. Anion inhibition of the proton pump in rat liver multivesicular bodies. *J. Biol. Chem.* 261:15941–15948.

Warren, J. R., and B. J. Marshall. 1983. Unidentified curved bacilli on gastric epithelium in active chronic gastritis. *Lancet.* 1:1273–1275.